Title page

Altered spontaneous activity and effective connectivity of the anterior cingulate cortex in obsessive-compulsive disorder

Running title: ALFF and EC alterations of ACC in OCD

Jingyi Long[1,2#], Lekai Luo[1,2#], Yi Guo[1,2], Wanfang You[1,2,3], Qian Li[1,2], Bin Li[4], Wanjie Tang[4], Yanchun Yang[4], Graham J. Kemp[5], John A. Sweeney[1,6], Fei Li[1,2*], Qiyong Gong[1,2*]

[1] Huaxi MR Research Center (HMRRC), Functional and Molecular Imaging Key Laboratory of Sichuan Province, Department of Radiology, West China Hospital of Sichuan University, Chengdu 610041, Sichuan, PR China.

[2] Psychoradiology Research Unit of Chinese Academy of Medical Sciences (2018RU011), West China Hospital of Sichuan University, Chengdu 610041, Sichuan, PR China.

[3] Medical Imaging Technology Department, West China School of Medicine, Sichuan University.

[4] Department of Psychiatry, West China Hospital of Sichuan University, Chengdu 610041, Sichuan, PR China.

[5] Liverpool Magnetic Resonance Imaging Centre (LiMRIC) and Institute of Ageing and Chronic Disease, University of Liverpool, Liverpool, United Kingdom.

[6] Department of Psychiatry, University of Cincinnati, Cincinnati, OH, United States

[#] Jingyi Long and Lekai Luo contributed to the work equally.

[*]Corresponding authors: Fei Li, M.D., Ph.D. (charlie_lee@qq.com) and Qiyong Gong, M.D., Ph.D. (qiyonggong@hmrrc.org.cn), Huaxi MR Research Center (HMRRC), Functional and Molecular Imaging Key Laboratory of Sichuan Province, Department of Radiology, West China Hospital of Sichuan University, No. 37 Guo Xue Lane, Chengdu 610041, Sichuan, PR China.

Acknowledgements

This study was supported by the National Natural Science Foundation (Grant Nos. 81621003, 81761128023, 81820108018, 81227002 and 81401396), National Key Technologies R&D Program (Program No. 2012BAI01B03) and Program for Changjiang Scholars and Innovative Research Team in University (PCSIRT, Grant No. IRT16R52) of China. Dr. Gong would also like to acknowledge the support from his Changjiang Scholar Professorship Award (Award No. T2014190) of China and American CMB Distinguished Professorship Award (Award No. F510000/G16916411) administered by the Institute of International Education, USA. Dr. Li would like to acknowledge the support from the China Postdoctoral Science Foundation (2017T100699), Sichuan Science and Technology Program (2019YJ0098), Science and Technology Project of the Health Planning Committee of Sichuan (18ZD035), Technology Foundation for the Selected Returned Overseas Chinese Scholars (Sichuan Provincial Human Resources and Social

Security Department, [2018]145-19), and Fundamental Research Funds for the Central Universities (2018SCUH0011).

Conflict of Interest Statement

All authors declare no financial interests or potential conflicts of interest.

Author Contribution

FL, YCY, and QYG conceptualized the project. FL, JYL, and QYG designed the study and drafted the manuscript. FL, JYL, YG, QL, LKL, BL, and WJT contributed to literature search, data collection and analysis, as well as data interpretation. FL, GJK, JAS, and QYG critically revised the manuscript. All authors approved the final version of the manuscript.

Data Availability Statement

The data that support the findings of this study are available from the corresponding authors upon reasonable request.

Abstract

Obsessive-compulsive disorder (OCD) is a disabling neuropsychiatric disorder whose neurobiological basis remains unclear. Magnetic resonance imaging (MRI) studies have reported functional and structural alterations of the anterior cingulate cortex (ACC) in OCD. In this study we explored the functional activity of the ACC and effective connectivity (EC) between ACC and the whole brain in OCD to identify subregional ACC features that are altered and to investigate their impact on the region's EC with other brain structures. We performed resting-state functional MRI and Granger causality analysis (GCA) in 31 patients with OCD and 36 healthy controls, and analyzed the amplitude of low-frequency fluctuation (ALFF) and coefficient-based GCA. The left pregenual ACC (pACC) in patients with OCD showed decreased ALFF relative to controls (P=0.029). There were significantly decreased excitatory effects from the left pACC to both right dorsal superior frontal gyrus (dSFG) (P=0.016) and left precuneus (P=0.019) in patients compared with controls. Patients also showed a decreased inhibitory feedback flow from left ventral SFG to the left pACC than controls (P=0.029). The ALFF and EC results were validated and remained similar in subgroup analyses and in comparisons using the data without global signal regression. In patients, path coefficients from left pACC to right dSFG showed significant correlations with obsession (r=-0.387, P=0.031) and anxiety ratings (r=-0.422, P=0.018). In OCD, decreased spontaneous neural activity, altered EC of pACC with widely distributed cortical circuitry, and associations with clinical ratings highlight the importance of pregenual ACC functional alteration in OCD.

Keywords: Obsessive-compulsive disorder, resting-state functional MRI, Granger causality analysis, effective connectivity, anterior cingulate cortex, RRID:SCR_002372, RRID:SCR_002865, RRID:SCR_007037, RRID:SCR_009605, RRID:SCR_009641

1 Introduction

Obsessive-compulsive disorder (OCD) is a chronic, heritable, and disabling neuropsychiatric disorder with a lifetime prevalence of 2-3% (Menzies et al., 2008). Patients with OCD are characterized by intrusive thoughts and repetitive thoughts and behaviors (Hirschtritt, Bloch, & Mathews, 2017), resulting in an impaired quality of life. The neurobiological basis of OCD remains to be clarified, but converging neuroimaging and neuropsychological evidence implicate abnormalities in specific brain circuitry (Menzies et al., 2008), particularly specific loops in the cortico-striato-thalamo-cortical (CSTC) circuitry (Alexander, DeLong, & Strick, 1986; Graybiel & Rauch, 2000). The CSTC circuitry comprises a series of parallel yet integrated loops that topographically connect distinct regions of frontal cortex predominantly with striatum and thalamus (Haber, 2003; Haber & Knutson, 2010), as well as other regions including the amygdala, hippocampus and anterior cingulate cortex (ACC) (Menzies et al., 2008; Stern et al., 2013). Magnetic resonance imaging (MRI) studies have provided evidence of structural change in CSTC circuitry, notably abnormal gray matter volume in the ACC, prefrontal cortex, striatum and thalamus (Milad & Rauch, 2012). Functional MRI (fMRI) studies have demonstrated dysconnectivity within and between frontal and subcortical regions (Endrass & Ullsperger, 2014; Milad & Rauch, 2012). Beyond the classical theory of CSTC abnormality in OCD, recent studies highlight the role of widely-distributed abnormalities within large-scale intrinsic brain networks including the default mode network (DMN) and a fronto-parieto-limbic network (Anticevic et al., 2014; Gursel, Avram, Sorg, Brandl, & Koch, 2018).

The ACC is a key node within CSTC circuitry and belongs to other high-priority brain networks such as the DMN (Bush, Luu, & Posner, 2000). The ACC has 3 subdivisions: the pregenual, subgenual, and dorsal ACC. Broadly construed, the pregenual ACC (pACC) and subgenual ACC are considered to be an "affective subdivision" implicated in emotional responses, and the dorsal ACC (dACC) is the "cognitive subdivision" involved in response selection and cognitive processing (Pizzagalli, 2011). Functionally, the dACC is crucial in supporting error monitoring and behavioral flexibility in dynamically changing environments (D'Cruz, Ragozzino, Mosconi, Pavuluri, & Sweeney, 2011), which represent core neurocognitive abnormalities in OCD. Pregenual and subgenual divisions of ACC may contribute to affective features of the disorder. Indirectly supporting the ACC as a key node in OCD are the observations that stimulation of ACC can induce compulsive goal-directed behaviors and perseveration (Pizzagalli, 2011), that reduced volume of dACC in preschool children with exaggerated performance monitoring increases their risk for OCD (Gilbert, Barclay, Tillman, Barch, & Luby, 2018), and that partial surgical ablation of ACC can in some cases relieve symptoms in treatment-refractory OCD (Kim et al., 2003). More direct evidence includes fMRI observations in OCD of abnormal regional functional activity in ACC (Saxena, Brody, Schwartz, & Baxter, 1998; Saxena & Rauch, 2000) and altered functional connectivity (FC) between dACC and caudate, which has been related to symptom severity of OCD symptoms (Zhang et al., 2017). What has not so far been systematically studied in OCD are alterations in the effective connectivity of ACC subregions with widely distributed brain circuitry.

Typically, static FC analysis has been used to examine the correlations of activity across brain regions, but this does not provide information on the causal influence of one brain area on another (K. J. Friston, Frith, Liddle, & Frackowiak, 1993). Effective connectivity (EC) analysis was developed to address this issue of the directional influence of one region over another (Valdes-Sosa, Roebroeck, Daunizeau, & Friston, 2011). Estimates of EC typically derive from a generative model that provides a forward mapping from hidden neuronal circuit dynamics to observable brain signals (K. Friston, Moran, & Seth, 2013), which exhibits information about the directionality of effects so that it is possible to determine which brain region exerts influence or receives influence from another. Granger causality analysis (GCA) is a widely used computational method to calculate the EC of neural networks (Seth, Barrett, & Barnett, 2015). The basic idea behind GCA is that if x contains information that helps predict the future of y better than information in the past of y, we can conclude that x causes y. GCA uses systematic temporal differences in oscillations or event-related responses from time-series data in different regions to infer the direction and strength of the causal influence of regional neural activity (K. J. Friston, 2011; Valdes-Sosa et al., 2011), thus holding out the promise of determining whether the preceding neural activity in one seed region predicts subsequent activity in another region.

In OCD, 3 resting-state fMRI (rfMRI) studies using GCA have shown altered causal influences between the striatum and other areas of the CSTC circuitry (Abe et al., 2015; Dong et al., 2019; Xie et al., 2017) and 1 rfMRI study only considered causal connections between pACC and other CSTC regions (Tadayonnejad et al., 2018). By using dynamical

causal modeling (DCM), 1 study found task-related modulation of EC from the dorsal ACC to the left dorsolateral prefrontal cortex (DLPFC) in the incongruent task condition (Schlosser et al., 2010), and another task-based fMRI study showed a significantly altered EC between the ventromedial prefrontal cortex and the orbitofrontal cortex in a reward learning task (Alves-Pinto et al., 2019). However, these 6 EC studies in OCD had limitations. The results of task-based fMRI studies are not comparable due to different tasks and because they neglect the intrinsic functional influences among brain regions. In 2 rfMRI studies, patients with OCD also had comorbid psychiatric disorders such as major depression and anxiety disorders (Dong et al., 2019; Tadayonnejad et al., 2018). All these 4 rfMRI studies either did not report the excitatory or inhibitory influence of identified causal influences (Dong et al., 2019; Tadayonnejad et al., 2018; Xie et al., 2017) or only focused on excitatory effects (Abe et al., 2015), which may not reveal the full spectrum of causal influences between the ACC and other whole brain regions in OCD.

As a data-driven method, GCA computes the information flow based on the data itself at the level of seed regions and network, relies on fewer assumptions about the underlying interactions, and is less computationally intensive than other EC methods such as DCM (Chand & Dhamala, 2017; Stephan et al., 2010). Therefore, to explore whether, in OCD, the spontaneous activity of ACC subregions is abnormal, and neural function of ACC subregions is a primary abnormality or simply responds to abnormalities in other brain structures, we used rfMRI and GCA to investigate the intrinsic function of ACC subregions and the information flow between them and other brain regions in OCD. We hypothesized first that ACC subregions would show abnormal intrinsic spontaneous

activity, and the abnormal subregions would show significantly altered EC with brain regions not only in the CSTC circuitry but in other networks, such as DMN. Second, we hypothesized that these altered functional characteristics would be related to the clinical symptoms of OCD.

2 Materials and Methods

2.1 Subjects

The study was approved by the local research ethics committee, and written informed consent was obtained from all participants. A total of 31 patients with OCD were recruited (12 females; mean age [± standard deviation] 27.1 ± 9.5 years, range 16-52 years; mean education 13.7 ± 2.9 years, range 8-19 years; mean duration of illness 6.0 ± 5.4 years, range 1-23 years). Seventeen patients were drug-naive, while the remaining 14 previously received psychiatric medications (4 clomipramine, 4 paroxetine, 3 fluoxetine, and 3 sertraline) and had been medication free for more than 2 weeks. Patients with OCD were diagnosed using the Structured Clinical Interview for DSM-IV Axis I Disorders (SCID-I). Their predominant obsessions/compulsions were determined according to the five clinical dimensions defined by Mataix-Cols et al. (Mataix-Cols, Rauch, Manzo, Jenike, & Baer, 1999): 23 aggressive/checking, 5 contamination/cleaning, 2 symmetry/ordering and 1 sexual/religious, and none with hoarding symptoms. Clinical symptoms of patients with OCD were assessed using the Yale-Brown Obsessive-Compulsive Scale (Y-BOCS), the 14-item Hamilton Anxiety Rating Scale (HARS), and the 17-item Hamilton Depression Rating Scale (HDRS) (Table 1).

A total of 36 healthy controls (15 females; mean age 24.6 ± 7.4 years, range 18-44 years; mean education 13.3 ± 2.8 years, range 5-19 years) were evaluated using the SCID-I/NP (Non-patient Edition) to rule out current or past psychiatric disorders. Interviews with control participants revealed no history of psychiatric disorder in their first-degree

relatives. Exclusion criteria for both groups included: any neurological disorder, neurosurgery, current or past substance abuse or dependence, pregnancy, and magnetic resonance contraindications. MR images were inspected by 2 experienced neuroradiologists to confirm the absence of gross brain abnormalities. Thirty-one OCD patients and 36 controls did not differ significantly with respect to age ($P = 0.773$), gender ($P = 0.806$), and years of education ($P = 0.588$), and were all right-handed (Table 1).

2.2 Image acquisition and processing

Subjects underwent rfMRI with a 3T MR imaging system (Excite, GE) with an 8-channel phased-array head coil. They were instructed to relax with eyes closed and without falling asleep or systematic thought during scanning. MR images were obtained using a gradient-echo echo-planar imaging sequence with these parameters: repetition/echo time, 2000/30 msec; thickness, 5 mm, with no intersection gaps; flip angle, 90°; matrix size, 64×64; field of view, 240×240 mm^2; voxel size, 3.75×3.75×5 mm^3. Each volume comprised 30 axial sections to cover the whole brain, and each run contained 200 image volumes preceded by 5 dummy volumes, leading to a total scanning time of 410 seconds.

Using DPARSF software (RRID:SCR_002372), the first 5 volumes were discarded to allow the stabilization of longitudinal magnetization. The remaining images were realigned to the middle volume using a 6-parameter (rigid body) linear transformation. We then used the Friston 24-parameter model to regress out the potential effects of head motion from the realigned data (Yan et al., 2013). For all participants, the head translation

movement was < 1.5 mm and rotation < 1.5°. In the mean framewise displacement (FD) (Jenkinson) of head motion (Jenkinson, Bannister, Brady, & Smith, 2002), there was no significant difference between patients (0.046 mm ± 0.034) and controls (0.044 mm ± 0.020) (P = 0.773). Signals of white matter, global brain signals, and cerebrospinal fluid were regressed out in the main analyses. During this step, we retained the preprocessed rfMRI data both with and without global signal regression (GSR), and validated the main results, which were from the data with GSR, by using the data without GSR. Because the blood-oxygen-level-dependent (BOLD) signal can demonstrate low-frequency drift, we included a linear trend as a regressor. The resulting data were temporally bandpass-filtered (0.01-0.08Hz) to reduce high-frequency physiological noise. All images were then spatially normalized to the Montreal Neurologic Institute (MNI) template, each voxel was resampled to 3×3×3 mm^3, and a spatial smoothing transformation was performed with an 8-mm full-width half-maximum Gaussian kernel.

2.3 Amplitude of low-frequency fluctuations (ALFF) and GCA calculation

The ALFF represents the power in the BOLD signal within a specific low-frequency range, reflecting spontaneous neural activity (Fox & Raichle, 2007). ALFF was calculated using DPARSF software (RRID:SCR_002372). After data preprocessing, the time series for each voxel was transformed to the frequency domain, and the power spectrum was obtained; the power spectrum was square-root transformed and the averaged square root of power in the frequency band (0.01-0.08Hz) was taken as the ALFF. For each voxel, the

ALFF was standardized by dividing by the mean value of an individual across all voxels of their ALFF map.

Vector autoregressive models were used to assess Granger causality. We used signed-path coefficients (Hamilton, Chen, Thomason, Schwartz, & Gotlib, 2011; Palaniyappan, Simmonite, White, Liddle, & Liddle, 2013; Zang, Yan, Dong, Huang, & Zang, 2012) to infer the effects of physiological influences. In GCA, a significantly positive path coefficient (e.g. time series of a region [x] relative to another [y]) suggests an excitatory effect of region x on region y, while a significantly negative path coefficient indicates an inhibitory influence of region x on region y; we call these a driving effect/flow (x to y) and a vice versa feedback effect/flow (y to x), respectively. We performed first-order voxel-wise coefficient-based GCA using REST software (RRID:SCR_009641), which allows for bidirectional influences. The signed-path coefficient maps of GCA were used for parametric statistical analysis and group-level inference (Hamilton et al., 2011; Palaniyappan et al., 2013; Zang et al., 2012).

2.4 Statistical analysis

We compared patients and controls for age and years of education with a 2-sample *t*-test and for sex ratio with a chi-square analysis in SPSS software (RRID:SCR_002865). A 2-sample *t*-test was performed in SPM8 (RRID:SCR_007037) to explore the group differences in the ALFF of bilateral ACC. We used the bilateral ACC masks (including all 3 subdivisions) from the Automated Anatomical Labeling template as explicit masks

to restrict the analysis in ACC with a threshold of $P < 0.05$ corrected for multiple comparisons with the family-wise error (FWE) method at the cluster level.

Next, we selected clusters with altered ALFF within ACC in patients relative to controls as a seed and used the GCA method to explore the directional influence between the seed and the whole brain in a voxelwise manner. For both groups, the GCA maps were analyzed with a 1-sample *t*-test to identify voxels showing significant positive or negative Granger causality from and to the time-course of the seed, with voxel-level uncorrected $P < 0.001$ and cluster size of 19 to yield a cluster-level uncorrected $P < 0.05$. For between-group comparison, a 2-sample *t*-test was used to compare GCA maps with $P < 0.05$ corrected with FWE at the cluster level. The between-group comparison was restricted to the regions with excitatory or inhibitory influence from and to the seed in either patients or controls by using a mask that comprised the union set of 1-sample *t*-test results of the 2 groups.

The mean FD (Jenkinson), age, and sex was used as covariates in all group-level analyses. We reported the coordinates of regions with significant group differences in MNI space. When the group-comparison results were significant in a brain region, the values of ALFF and signed-path coefficients were extracted using the automated tool Marsbar (RRID:SCR_009605). In the patient group, Pearson correlation analysis was performed to investigate the relationship between the ALFF and EC findings with the clinical variables (including illness duration and scores from Y-BOCS, HARS, and HDRS). Nominal significance thresholds were used for these exploratory/heuristic

correlation analyses ($P < 0.05$).

3 Results

3.1 Between-group differences in ALFF

Compared with the controls, patients with OCD showed significantly decreased ALFF in the left pACC (Brodmann area 32; MNI coordinates: -9, 39, 3; cluster size = 54 voxels; peak $t = 4.08$; $P = 0.029$ at cluster level, FWE corrected) (Table 4a and Figure 1a). There were no regions with significantly increased ALFF in bilateral ACC.

3.2 Within-group patterns of GCA

The left pACC *exerted an excitatory influence* (the path coefficient is significantly > 0) on the right dorsal superior frontal gyrus (dSFG), bilateral caudate and thalamus, posterior cingulate cortex (PCC), and precuneus in controls, and on bilateral caudate and medial prefrontal cortex (mPFC) in patients with OCD. The left pACC *exerted an inhibitory effect* (path coefficient significantly < 0) on the right inferior temporal gyrus and middle frontal gyrus, left medial temporal gyrus and orbitofrontal cortex in both groups, and also on the right insular, bilateral supramarginal gyrus and cerebellum in controls (Table 2a and Figure 2a).

The left pACC *received an excitatory influence* (path coefficient significantly > 0) from bilateral medial temporal gyrus and right cerebellum in both groups, and from bilateral supramarginal gyrus and left cerebellum in controls. The left pACC *received an inhibitory influence* (path coefficient significantly < 0) from the bilateral dorsolateral

prefrontal cortex, PCC and precuneus, and left ventral superior frontal gyrus (vSFG) in controls, and from bilateral caudate and mPFC in patients (Table 3a and Figure 3a).

3.3 Between-group differences in GCA

There was a significant difference between patients with OCD and controls in the driving effect from the left pACC to the right dSFG ($P = 0.016$) (Table 4a and Figure 1b): there was mainly an excitatory influence (path coefficient =1.27±1.6) in controls, but mainly an inhibitory influence (path coefficient =-0.09±1.4) in patients. In the patient group, the path coefficient of driving effect from the left pACC to the right dSFG showed significant negative correlations with the obsessive subscale scores of Y-BOCS ($r = -0.387$, $P = 0.031$) and HARS scores ($r = -0.422$, $P = 0.018$). In addition, there was a significant between-group difference in the driving effect of the left pACC to the left precuneus ($P = 0.019$) (Table 4a and Figure 1c): there was mainly an excitatory influence (path coefficient =1.51±2.08) in controls, but mainly an inhibitory influence (path coefficient =-0.16±1.87) in patients. Thus, patients with OCD had decreased driving effects (less excitatory influence) from the left pACC to the right dSFG and left precuneus than controls, respectively (Figure 1e).

Patients also showed a significantly greater feedback influence from the left vSFG to the left pACC (path coefficient = 0.42 ± 1.06) compared with controls (path coefficient = -0.68 ± 1.09) ($P = 0.029$) (Table 4a and Figure 1d), suggesting a reduced inhibitory influence from the left vSFG to the left pACC in patients with OCD relative to controls

(Figure 1e).

3.4 Subgroup analyses among drug-naive and drug-free patients and controls

After extracting the value of ALFF in left pACC and path coefficient of GCA from the left pACC to right dSFG and to the left precuneus and from left vSFG to left pACC, respectively, for every subject, a one-way analysis of variance followed by pair-wise comparisons with Bonferroni correction comparing drug-naive patients (n = 17), previously medication-treated patients (n = 14), and controls (n = 36) revealed similar group differences in ALFF and EC parameters (see below) as seen in the comparisons between all the patients pooled and controls (Figure 4a). No significant differences were observed between the 2 patient subgroups.

For the ALFF value of left pACC, we found a significant difference ($F = 11.001$, $P < 0.001$) among the 3 groups. The values of ALFF between 2 subgroups of patients with OCD did not differ ($P = 0.776$) and both subgroups had decreased ALFF in the left pACC relative to controls (drug-naive patients, Cohen's $d = 0.92$, $P = 0.007$; previously treated patients, Cohen's $d = 1.42$, $P < 0.001$).

For the driving effect from the left pACC to right dSFG, we found a significant difference ($F = 7.015$, $P = 0.002$) among 3 groups. The path coefficient of EC from the left pACC to right dSFG in the 2 subgroups of patients with OCD did not differ ($P = 1$) and both subgroups had decreased path coefficient of EC from the left pACC to right

dSFG relative to controls (drug-naive patients, Cohen's $d = 0.81$, $P = 0.032$; previously treated patients, Cohen's $d = 1.01$, $P = 0.004$).

For the driving effect from the left pACC to the left precuneus, we found a significant difference ($F = 6.01$, $P = 0.004$) among the 3 groups. The path coefficient of EC from left pACC to left precuneus between 2 subgroups of patients with OCD did not differ ($P = 1$) and both subgroups had decreased path coefficient of EC from left pACC to right dSFG relative to controls (drug-naive patients, Cohen's $d = 0.88$, $P = 0.007$; previously treated patients, Cohen's $d = 0.79$, $P = 0.045$).

For the feedback influence from left vSFG to left pACC, we found a significant difference ($F = 9.229$, $P < 0.001$) among the 3 groups. The path coefficient of EC from the left vSFG to the left pACC between 2 subgroups of patients with OCD did not differ ($P = 0.993$) and both subgroups had increased path coefficients of EC from the left vSFG to left pACC relative to controls (drug-naive patients, Cohen's $d = 1.2$, $P < 0.001$; previously treated patients, Cohen's $d = 0.81$, $P = 0.031$).

3.5 Subgroup analyses for adult patients

There were 2 late adolescent patients, of whom one was 16 and the other 17 years old. We repeated all the analyses with only the 29 adult patients with OCD (12 females; mean age 27.8 ± 9.4 years, range 18-52 years; mean education 13.9 ± 2.9 years, range 8-19 years; FD 0.043 mm ± 0.031) and all 36 adult healthy controls, in which the 2 groups did

not differ significantly with respect to age (P = 0.246), gender (P = 0.554) or years of education (P = 0.342), FD (P = 0.399), and were all right-handed. We performed 2-sample *t*-tests for ALFF and GCA maps in SPM8 (RRID:SCR_007037) using the same covariates and threshold as those in the main results. The statistical comparisons of 29 adult patients with OCD and 36 controls revealed similar group differences in ALFF and EC parameters as seen in the comparisons between all the 31 patients pooled and controls (Table 4b and Figure 4b).

3.6 Results from data without GSR

Since previous studies showed that anticorrelations were mathematically mandated by GSR, rendering them uninterpretable, and caused spurious correlations using GSR in addressing physiological aliasing confounds (Murphy, Birn, Handwerker, Jones, & Bandettini, 2009; Saad et al., 2012), we repeated all the statistical comparisons between 31 patients and 36 controls using data without GSR, with the same covariates and threshold as those in the main results.

For the driving effect: the within-group results from the data without GSR demonstrated that the left pACC exerted significant inhibitory effects on bilateral occipital lobe and right superior parietal lobule (SPL) in controls and on bilateral SPL in patients, which were not shown in the results from the data with GSR. The inhibitory effect of pACC on bilateral temporal gyrus in patients using data with GSR was not found in the within-group results using data without GSR (Table 2b and Figure 2b).

For the feedback effect: the excitatory effect of the cerebellum on pACC in both groups using data with GSR was not shown in the results using data without GSR. The excitatory effect of inferior frontal gyrus on pACC in both groups and the inhibitory effect of bilateral occipital lobe on pACC in patients were shown in the results using data without GSR (Table 3b and Figure 3b).

Besides these differences between the results found using the data with and without GSR, the results of the within-group 1-sample *t*-tests using data with GSR remained similar in the results from the data without GSR in both groups. Using the data without GSR, the 2-group comparisons of ALFF and GCA showed similar results to the main findings, with additional decreased inhibitory feedback flow from the left thalamus and caudate to the left pACC in patients compared to controls (Table 4c and Figure 4c).

4 Discussion

There are 4 major findings in this study of ACC function and effective connectivity in OCD: 1) decreased ALFF in the left pACC; 2) decreased excitatory influence from the left pACC to the right dSFG and left precuneus; 3) decreased inhibitory feedback effect from the left vSFG to the left pACC; and 4) significant correlations between the signed-path coefficient from the left pACC to the right dSFG and clinical variables (the obsessive subscale scores of Y-BOCS and HARS scores). These findings advance understanding of the importance and consequences of pACC dysfunction both within and outside the classic CSTC circuitry and suggest that the altered EC within the frontal lobe might be critical in the pathophysiology of OCD.

4.1 Decreased ALFF in pACC

Compared with controls, patients showed decreased ALFF (i.e. less spontaneous neuronal activity) in the left pACC. The pACC is an affective part of ACC and plays a key role in emotional processing, affect regulation, and pain perception (Pizzagalli, 2011; Shackman et al., 2011). Our findings parallel other evidence of pACC pathophysiology in OCD. Structural MRI studies have reported decreased gray matter volume (Carlisi et al., 2017) and cortical thickness (Cavanagh, Grundler, Frank, & Allen, 2010) in the pACC, the latter correlating with a greater reduction in Y-BOCS scores after exposure therapy (Fullana et al., 2014). fMRI studies revealed hypoactivation of pACC during tasks of interference inhibition and task switching (Weidt et al., 2016). MR spectroscopy studies report lower

levels in the pACC of neurotransmitters such as N-acetylaspartate (NAA) (Weber et al., 2014), glutamate and glutamine (O'Neill et al., 2016; Rosenberg et al., 2004; Tadayonnejad et al., 2018), these decreases being significantly correlated with clinical symptoms of OCD (Yucel et al., 2008).

Interestingly, in OCD the pACC exhibits increased functional activity during response-conflict tasks designed to elicit errors (Agam et al., 2014; Fitzgerald et al., 2005; Riesel, Endrass, Kaufmann, & Kathmann, 2011), and hyperactivity with subthreshold stimulation (Jocham & Ullsperger, 2009). Patients with OCD are often reported to have increased performance monitoring activity (Hoffmann & Falkenstein, 2012; Mathews, Perez, Delucchi, & Mathalon, 2012), which reflects concerns driving obsessions and compulsions (Debener et al., 2005; Endrass & Ullsperger, 2014) and has been considered to be an endophenotype of OCD (Gilbert et al., 2018; Riesel et al., 2011). Error-related brain activity can be assessed in an event-related electroencephalogram by the error-related negativity (ERN), which is a validated marker of performance monitoring (Debener et al., 2005; Fitzgerald et al., 2005). The ACC is the generator of ERN, and increased ERN has been found in the ACC (specifically, the pACC) in patients with OCD (Debener et al., 2005; Fitzgerald et al., 2005; Mathews et al., 2012). Thus, pACC activity, elevated in task states and decreased in the resting state, may reflect how patients with OCD deal with conflict: as they over-evaluate possible conflict responses the pACC receives intensive error-related stimulation, leading to elevated task-related activity and generating ERN amplitudes. In the resting state, the intrinsic functional activity and metabolism of pACC may be decreased, perhaps reflecting recovery or increased

inhibitory input following excessive activation. Thus, the pACC may be a site of vulnerability or regional pathology in patients with OCD, with an increase in the excitatory/inhibitory neuronal balance with different alterations seen during exaggerated performance monitoring and reduced activity during the resting state.

4.2 Altered EC in the CSTC circuitry

There were significantly decreased excitatory effects from the left pACC to right dSFG, and decreased inhibitory feedback flow from left vSFG to the left pACC in patients with OCD. The pACC and SFG are part of the CSTC circuitry. The SFG, the superior part of the prefrontal cortex, has several subregions involved in cognitive control tasks; both the dSFG and vSFG are engaged in cognitive control processes (Li et al., 2013). Several studies in OCD have found structural and functional abnormalities of SFG in OCD (Fan et al., 2018; Nakao et al., 2005; Simon, Adler, Kaufmann, & Kathmann, 2014), including decreased gray matter volume (Carlisi et al., 2017), lower task-related functional activity (Kocak, Ozpolat, Atbasoglu, & Cicek, 2011), and decreased FC with the pACC (Zhang et al., 2017). Our finding of altered information flow between the pACC and SFG supports the importance of altered functional integration within CSTC circuitry in OCD. Causally, the decreased excitatory influence from left pACC to the right dSFG may be attributed to the decreased spontaneous functional activity of the left pACC, while the smaller inhibitory influence from the left vSFG to the left pACC may represent functional compensation in OCD.

In our patient group, the path coefficient from the left pACC to the right dSFG was negatively correlated with Y-BOCS obsessive subscale scores, indicating that the lower the signed path coefficient of the causal effect, the worse the clinical symptoms. A PET study of the therapeutic effects of anterior capsulotomy reported that the more the metabolism in the bilateral ACC and SFG decreased after capsulotomy, the more the Y-BOCS scores improved (Zuo et al., 2013). Our correlation results support an important role of these 2 regions in the pathophysiology of OCD. OCD has high comorbidity with anxiety disorders (Swartz et al., 2014; Weidt et al., 2016), and the intrusive thoughts and repetitive behaviors in OCD may in part represent efforts to reduce anxiety generated by obsessions (Hirschtritt et al., 2017). Hypoactivation in the pACC in anxiety disorders may reflect its inadequate performance in regulating attention (Swartz et al., 2014; Weidt et al., 2016). The negative correlation between HARS scores and the path coefficient of GCA (greater anxiety is associated with lower driving effect from left pACC to right dSFG) suggests that this pathway may serve as a potential pathophysiological feature in OCD.

Besides the EC between ACC and SFG, previous studies had found other EC alternations in CSTC circuitry. Three rfMRI studies using selected striatum regions as seeds found altered EC between striatum regions and frontal areas in patients with OCD (Abe et al., 2015; Dong et al., 2019; Xie et al., 2017). A task-based study selected dorsal ACC and rostral ACC as nodes, and found enhanced task-related modulation of EC from the dorsal ACC to the left DLPFC (Schlosser et al., 2010). Together with our results, these studies support the idea that abnormalities in specific loops in the CSTC circuitry play

the important role in the neurobiology of OCD (Alexander et al., 1986; Graybiel & Rauch, 2000). One rfMRI study also selected bilateral pACC regions as seeds, finding that the feedback influence of the right dorsal anterior midcingulate cortex on the right pACC was decreased, which correlated with depression symptoms of OCD (Tadayonnejad et al., 2018). In contrast we did not find EC alteration between pACC and other subregions of cingulate cortex: this difference might be explained by the comorbid depression in the patient group studied by Tadayonnejad et al., or the lower resolution of data in the present study.

Whether with or without using GSR for the data preprocessing, in controls the left pACC exerted a significant excitatory influence on thalamus/caudate, and the thalamus/caudate exerted a significant inhibitory effect on the left pACC; this may represent a normal pattern of EC between pACC and thalamus/caudate keeping the functional stability between these regions in the CSTC circuit. Although this pattern still existed in OCD, our finding using the data without GSR supported the idea that an attenuated thalamus/caudate-to-pACC inhibitory effect has an important role in OCD. The thalamus acts as a central convergent hub for the rest of the brain, and nerve fibers project out of the thalamus to the cerebral cortex including the ACC (Ward, 2013). The caudate interconnects with the ACC and other cortical networks, and dysfunction of caudate and associated cortico-striatum circuits is considered to be a common neural feature of OCD (Graybiel & Rauch, 2000). This is consistent with reports of decreased volume in thalamus (Tang et al., 2016) and left striatum (Dogan, Ertekin, Turkdogan, Memis, & Sevincok, 2019) in OCD. They also parallel the findings from fMRI studies in

OCD which found decreased fractional ALFF (Qiu et al., 2017) and regional homogeneity (Niu et al., 2017) in thalamus, and decreased ALFF in caudate (Tang et al., 2016), the hypofunction of which were correlated with symptom severity of OCD (Dogan et al., 2019; Qiu et al., 2017). This might lead to the attenuated inhibitory influence of the left thalamus/caudate on the left pACC in the present study.

Regarding the technical issue of GSR, Hannes et al. founded small or negligible to effects of GSR on EC, and reported that data without GSR were more informative, while the precision of posterior estimates was greater after GSR (Almgren, Van de Steen, Razi, Friston, & Marinazzo, 2020). Since the influence of GSR on analysis of fMRI data remains a topic of debate, the present results should be treated with caution.

4.3 Altered EC in DMN

We also found less excitatory influence from the left pACC to the left precuneus in the OCD group. The precuneus in the medial parietal cortex is believed to be involved in higher-order cognitive functions including self-centered mental imagery and episodic memory retrieval (Cavanna & Trimble, 2006). Disruption in episodic memory is one of the most consistent neuropsychological findings in OCD (Savage et al., 2000). A popular explanation considers that memory deficits in OCD are related to the encoding/acquisition stage of memory, in which patients fail to ignore irrelevant information during encoding, resulting in impaired retrieval of relevant content (Konishi, Shishikura, Nakaaki, Komatsu, & Mimura, 2011). Previous studies have confirmed the

extensive anatomical and functional connections between the precuneus and ACC, both of which are implicated in the classic episodic memory network (Batistuzzo et al., 2015; Cavanna & Trimble, 2006). Our finding of decreased inhibitory influence from the pACC to precuneus may, therefore, reflect the impairment of episodic memory retrieval in OCD. Further studies using GCA focusing on episodic memory retrieval are needed to test this hypothesis.

The DMN is a group of highly-interacting brain regions serving as the neurological basis for a variety of self-referential processes (Andrews-Hanna, 2012), which includes both the ACC and precuneus. The anteromedial SFG is also considered a part of DMN since it has an anatomical connection with the ACC through the cingulum and is functionally correlated with areas in the DMN (Li et al., 2013). In OCD, DMN alteration is hypothesized to mediate difficulties in sustaining attention toward external stimuli and disengaging from internally generated obsessional thoughts (Norman et al., 2017). rfMRI studies in OCD report widespread increased FC (mainly between the anteromedial SFG and the mid-cingulate cortex) (Hou et al., 2012) or functional dysconnectivity (between the ventromedial prefrontal cortex and the ACC) (Gursel et al., 2018) within the DMN, indicating an impaired balance between internally and externally focused thought in patients (Jang et al., 2011). Adding to these non-directional FC findings with our EC analysis, we found aberrant causal information flow within DMN regions, i.e. an abnormal driving influence of the left pACC on the left precuneus in OCD patients. This suggests a causal connectivity-based pathophysiologic process in OCD highlighting the role of pACC pathology. Notably, this EC alteration impacted not only CSTC circuitry in

OCD which is the major circuitry in current network models but also the DMN.

4.4 Limitations

Our sample size of patients was relatively small, and 14 out of 31 patients were previously receiving psychopharmacological treatment, which may be a confounding factor due to potential drug effects on brain function. Although we reported no significant differences in ALFF and path coefficient of EC between drug-naive and currently off-medication patients with OCD, the potential influences of prior medication on brain function could not be completely excluded. Longitudinal studies with controlled treatment are needed to establish medication effects on parameters investigated in the present study. Studies with larger samples may have more power needed to detect more subtle effects in regional ALFF change or EC. Second, we found decreased ALFF and disturbed EC of pACC and significant correlations between Granger causality metrics from pACC to dSFG and obsession and anxiety ratings in patients with OCD. However, structural and functional deficits of pACC have also been reported in other psychiatric disorders (Rosenberg et al., 2004; Swartz et al., 2014; Weidt et al., 2016). Further research is needed to explore whether the ALFF of pACC and alterations of modulation by pACC of SFG and precuneus are specific to OCD or are transdiagnostic features reflecting general psychopathology. This may be of particular interest regarding disorders such as autism where repetitive thinking and behavior are also common and related to ACC dysfunction (D'Cruz, Mosconi, Ragozzino, Cook, & Sweeney, 2016). From the methodological point

of view, the resolution of rfMRI data in our study is relatively low. Further research with a 32- or 64-channel head coil and multi-band accelerated echo-planar imaging sequences will be needed. Another issue is GSR in data preprocessing. Although previous studies showed that anticorrelations and aliasing confounds might be caused by GSR, we found similar and comparable results using data with and without GSR. It remains controversial whether GSR is necessary for rfMRI data. Further work is needed, and different preprocessing approaches might offer complementary information about the brain's functional organization (Murphy & Fox, 2017).

5 Conclusion

In summary, in patients with OCD, the pACC had decreased ALFF, and its altered Granger causality effect with components of neural networks including the CSTC and DMN suggests that pACC might be a primary functional abnormality underlying the pathophysiology of OCD. Supporting this idea is the correlation between the GCA results from the left pACC to the right dSFG and its relation to clinical symptom ratings.

Reference

Abe, Y., Sakai, Y., Nishida, S., Nakamae, T., Yamada, K., Fukui, K., & Narumoto, J. (2015). Hyper-influence of the orbitofrontal cortex over the ventral striatum in obsessive-compulsive disorder. *Eur Neuropsychopharmacol, 25*(11), 1898-1905. doi:10.1016/j.euroneuro.2015.08.017

Agam, Y., Greenberg, J. L., Isom, M., Falkenstein, M. J., Jenike, E., Wilhelm, S., & Manoach, D. S. (2014). Aberrant error processing in relation to symptom severity in obsessive-compulsive disorder: A multimodal neuroimaging study. *Neuroimage Clin, 5*, 141-151. doi:10.1016/j.nicl.2014.06.002

Alexander, G. E., DeLong, M. R., & Strick, P. L. (1986). Parallel organization of functionally segregated circuits linking basal ganglia and cortex. *Annu Rev Neurosci, 9*, 357-381. doi:10.1146/annurev.ne.09.030186.002041

Almgren, H., Van de Steen, F., Razi, A., Friston, K., & Marinazzo, D. (2020). The effect of global signal regression on DCM estimates of noise and effective connectivity from resting state fMRI. *Neuroimage, 208*, 116435. doi:10.1016/j.neuroimage.2019.116435

Alves-Pinto, A., Rus, O. G., Reess, T. J., Wohlschlager, A., Wagner, G., Berberich, G., & Koch, K. (2019). Altered reward-related effective connectivity in obsessive-compulsive disorder: an fMRI study. *J Psychiatry Neurosci, 44*(6), 395-406. doi:10.1503/jpn.180195

Andrews-Hanna, J. R. (2012). The brain's default network and its adaptive role in internal mentation. *Neuroscientist, 18*(3), 251-270. doi:10.1177/1073858411403316

Anticevic, A., Hu, S., Zhang, S., Savic, A., Billingslea, E., Wasylink, S., . . . Pittenger, C. (2014). Global resting-state functional magnetic resonance imaging analysis identifies frontal cortex, striatal, and cerebellar dysconnectivity in obsessive-compulsive disorder. *Biol Psychiatry, 75*(8), 595-605. doi:10.1016/j.biopsych.2013.10.021

Batistuzzo, M. C., Balardin, J. B., Martin Mda, G., Hoexter, M. Q., Bernardes, E. T., Borcato, S., . . . Miotto, E. C. (2015). Reduced prefrontal activation in pediatric patients with obsessive-compulsive disorder during verbal episodic memory encoding. *J Am Acad Child Adolesc Psychiatry, 54*(10), 849-858. doi:10.1016/j.jaac.2015.06.020

Bush, G., Luu, P., & Posner, M. I. (2000). Cognitive and emotional influences in anterior cingulate cortex. *Trends Cogn Sci, 4*(6), 215-222.

Carlisi, C. O., Norman, L. J., Lukito, S. S., Radua, J., Mataix-Cols, D., & Rubia, K. (2017). Comparative Multimodal Meta-analysis of Structural and Functional Brain Abnormalities in Autism Spectrum Disorder and Obsessive-Compulsive Disorder. *Biol Psychiatry, 82*(2), 83-102. doi:10.1016/j.biopsych.2016.10.006

Cavanagh, J. F., Grundler, T. O., Frank, M. J., & Allen, J. J. (2010). Altered cingulate sub-region activation accounts for task-related dissociation in ERN amplitude as a function of obsessive-compulsive symptoms. *Neuropsychologia, 48*(7), 2098-2109. doi:10.1016/j.neuropsychologia.2010.03.031

Cavanna, A. E., & Trimble, M. R. (2006). The precuneus: a review of its functional

anatomy and behavioural correlates. *Brain, 129*(Pt 3), 564-583. doi:10.1093/brain/awl004

Chand, G. B., & Dhamala, M. (2017). Interactions between the anterior cingulate-insula network and the fronto-parietal network during perceptual decision-making. *Neuroimage, 152*, 381-389. doi:10.1016/j.neuroimage.2017.03.014

D'Cruz, A. M., Mosconi, M. W., Ragozzino, M. E., Cook, E. H., & Sweeney, J. A. (2016). Alterations in the functional neural circuitry supporting flexible choice behavior in autism spectrum disorders. *Transl Psychiatry, 6*(10), e916. doi:10.1038/tp.2016.161

D'Cruz, A. M., Ragozzino, M. E., Mosconi, M. W., Pavuluri, M. N., & Sweeney, J. A. (2011). Human reversal learning under conditions of certain versus uncertain outcomes. *Neuroimage, 56*(1), 315-322. doi:10.1016/j.neuroimage.2011.01.068

Debener, S., Ullsperger, M., Siegel, M., Fiehler, K., von Cramon, D. Y., & Engel, A. K. (2005). Trial-by-trial coupling of concurrent electroencephalogram and functional magnetic resonance imaging identifies the dynamics of performance monitoring. *J Neurosci, 25*(50), 11730-11737. doi:10.1523/JNEUROSCI.3286-05.2005

Dogan, B., Ertekin, E., Turkdogan, F. T., Memis, C. O., & Sevincok, L. (2019). Cortico-thalamo-striatal circuit components' volumes and their correlations differ significantly among patients with obsessive-compulsive disorder: a case-control MRI study. *Psychiatry and Clinical Psychopharmacology, 29*(2), 162-170. doi:10.1080/24750573.2019.1583481

Dong, C., Yang, Q., Liang, J., Seger, C. A., Han, H., Ning, Y., . . . Peng, Z. (2019). Impairment in the goal-directed corticostriatal learning system as a biomarker for obsessive-compulsive disorder. *Psychol Med*, 1-11. doi:10.1017/S0033291719001429

Endrass, T., & Ullsperger, M. (2014). Specificity of performance monitoring changes in obsessive-compulsive disorder. *Neurosci Biobehav Rev, 46 Pt 1*, 124-138. doi:10.1016/j.neubiorev.2014.03.024

Fan, J., Gan, J., Liu, W., Zhong, M., Liao, H., Zhang, H., . . . Zhu, X. (2018). Resting-State Default Mode Network Related Functional Connectivity Is Associated With Sustained Attention Deficits in Schizophrenia and Obsessive-Compulsive Disorder. *Front Behav Neurosci, 12*, 319. doi:10.3389/fnbeh.2018.00319

Fitzgerald, K. D., Welsh, R. C., Gehring, W. J., Abelson, J. L., Himle, J. A., Liberzon, I., & Taylor, S. F. (2005). Error-related hyperactivity of the anterior cingulate cortex in obsessive-compulsive disorder. *Biol Psychiatry, 57*(3), 287-294. doi:10.1016/j.biopsych.2004.10.038

Fox, M. D., & Raichle, M. E. (2007). Spontaneous fluctuations in brain activity observed with functional magnetic resonance imaging. *Nat Rev Neurosci, 8*(9), 700-711. doi:10.1038/nrn2201

Friston, K., Moran, R., & Seth, A. K. (2013). Analysing connectivity with Granger causality and dynamic causal modelling. *Current Opinion in Neurobiology, 23*(2), 172-178. doi:10.1016/j.conb.2012.11.010

Friston, K. J. (2011). Functional and effective connectivity: a review. *Brain Connect, 1*(1), 13-36. doi:10.1089/brain.2011.0008

Friston, K. J., Frith, C. D., Liddle, P. F., & Frackowiak, R. S. (1993). Functional connectivity: the principal-component analysis of large (PET) data sets. *J Cereb Blood Flow Metab, 13*(1), 5-14. doi:10.1038/jcbfm.1993.4

Fullana, M. A., Cardoner, N., Alonso, P., Subira, M., Lopez-Sola, C., Pujol, J., . . . Soriano-Mas, C. (2014). Brain regions related to fear extinction in obsessive-compulsive disorder and its relation to exposure therapy outcome: a morphometric study. *Psychol Med, 44*(4), 845-856. doi:10.1017/S0033291713001128

Gilbert, K. E., Barclay, M. E., Tillman, R., Barch, D. M., & Luby, J. L. (2018). Associations of Observed Performance Monitoring During Preschool With Obsessive-Compulsive Disorder and Anterior Cingulate Cortex Volume Over 12 Years. *JAMA Psychiatry, 75*(9), 940-948. doi:10.1001/jamapsychiatry.2018.1805

Graybiel, A. M., & Rauch, S. L. (2000). Toward a neurobiology of obsessive-compulsive disorder. *Neuron, 28*(2), 343-347. doi:10.1016/s0896-6273(00)00113-6

Gursel, D. A., Avram, M., Sorg, C., Brandl, F., & Koch, K. (2018). Frontoparietal areas link impairments of large-scale intrinsic brain networks with aberrant fronto-striatal interactions in OCD: a meta-analysis of resting-state functional connectivity. *Neurosci Biobehav Rev, 87*, 151-160. doi:10.1016/j.neubiorev.2018.01.016

Haber, S. N. (2003). The primate basal ganglia: parallel and integrative networks. *J Chem Neuroanat, 26*(4), 317-330. doi:10.1016/j.jchemneu.2003.10.003

Haber, S. N., & Knutson, B. (2010). The reward circuit: linking primate anatomy and human imaging. *Neuropsychopharmacology, 35*(1), 4-26. doi:10.1038/npp.2009.129

Hamilton, J. P., Chen, G., Thomason, M. E., Schwartz, M. E., & Gotlib, I. H. (2011). Investigating neural primacy in Major Depressive Disorder: multivariate Granger causality analysis of resting-state fMRI time-series data. *Mol Psychiatry, 16*(7), 763-772. doi:10.1038/mp.2010.46

Hirschtritt, M. E., Bloch, M. H., & Mathews, C. A. (2017). Obsessive-Compulsive Disorder: Advances in Diagnosis and Treatment. *JAMA, 317*(13), 1358-1367. doi:10.1001/jama.2017.2200

Hoffmann, S., & Falkenstein, M. (2012). Predictive information processing in the brain: errors and response monitoring. *Int J Psychophysiol, 83*(2), 208-212. doi:10.1016/j.ijpsycho.2011.11.015

Hou, J., Wu, W., Lin, Y., Wang, J., Zhou, D., Guo, J., . . . Li, H. (2012). Localization of cerebral functional deficits in patients with obsessive-compulsive disorder: a resting-state fMRI study. *J Affect Disord, 138*(3), 313-321. doi:10.1016/j.jad.2012.01.022

Jang, J. H., Jung, W. H., Kang, D. H., Byun, M. S., Kwon, S. J., Choi, C. H., & Kwon, J. S. (2011). Increased default mode network connectivity associated with meditation. *Neurosci Lett, 487*(3), 358-362. doi:10.1016/j.neulet.2010.10.056

Jenkinson, M., Bannister, P., Brady, M., & Smith, S. (2002). Improved optimization for the robust and accurate linear registration and motion correction of brain images. *Neuroimage, 17*(2), 825-841.

Jocham, G., & Ullsperger, M. (2009). Neuropharmacology of performance monitoring.

Neurosci Biobehav Rev, 33(1), 48-60. doi:10.1016/j.neubiorev.2008.08.011

Kim, C. H., Chang, J. W., Koo, M. S., Kim, J. W., Suh, H. S., Park, I. H., & Lee, H. S. (2003). Anterior cingulotomy for refractory obsessive-compulsive disorder. *Acta Psychiatr Scand, 107*(4), 283-290. doi:10.1034/j.1600-0447.2003.00087.x

Kocak, O. M., Ozpolat, A. Y., Atbasoglu, C., & Cicek, M. (2011). Cognitive control of a simple mental image in patients with obsessive--compulsive disorder. *Brain Cogn, 76*(3), 390-399. doi:10.1016/j.bandc.2011.03.020

Konishi, M., Shishikura, K., Nakaaki, S., Komatsu, S., & Mimura, M. (2011). Remembering and forgetting: directed forgetting effect in obsessive-compulsive disorder. *Neuropsychiatr Dis Treat, 7*, 365-372. doi:10.2147/NDT.S21047

Li, W., Qin, W., Liu, H., Fan, L., Wang, J., Jiang, T., & Yu, C. (2013). Subregions of the human superior frontal gyrus and their connections. *Neuroimage, 78*, 46-58. doi:10.1016/j.neuroimage.2013.04.011

Mataix-Cols, D., Rauch, S. L., Manzo, P. A., Jenike, M. A., & Baer, L. (1999). Use of factor-analyzed symptom dimensions to predict outcome with serotonin reuptake inhibitors and placebo in the treatment of obsessive-compulsive disorder. *Am J Psychiatry, 156*(9), 1409-1416. doi:10.1176/ajp.156.9.1409

Mathews, C. A., Perez, V. B., Delucchi, K. L., & Mathalon, D. H. (2012). Error-related negativity in individuals with obsessive-compulsive symptoms: toward an understanding of hoarding behaviors. *Biol Psychol, 89*(2), 487-494. doi:10.1016/j.biopsycho.2011.12.018

Menzies, L., Chamberlain, S. R., Laird, A. R., Thelen, S. M., Sahakian, B. J., & Bullmore, E. T. (2008). Integrating evidence from neuroimaging and neuropsychological studies of obsessive-compulsive disorder: the orbitofronto-striatal model revisited. *Neurosci Biobehav Rev, 32*(3), 525-549. doi:10.1016/j.neubiorev.2007.09.005

Milad, M. R., & Rauch, S. L. (2012). Obsessive-compulsive disorder: beyond segregated cortico-striatal pathways. *Trends Cogn Sci, 16*(1), 43-51. doi:10.1016/j.tics.2011.11.003

Murphy, K., Birn, R. M., Handwerker, D. A., Jones, T. B., & Bandettini, P. A. (2009). The impact of global signal regression on resting state correlations: are anti-correlated networks introduced? *Neuroimage, 44*(3), 893-905. doi:10.1016/j.neuroimage.2008.09.036

Murphy, K., & Fox, M. D. (2017). Towards a consensus regarding global signal regression for resting state functional connectivity MRI. *Neuroimage, 154*, 169-173. doi:10.1016/j.neuroimage.2016.11.052

Nakao, T., Nakagawa, A., Yoshiura, T., Nakatani, E., Nabeyama, M., Yoshizato, C., . . . Kanba, S. (2005). Brain activation of patients with obsessive-compulsive disorder during neuropsychological and symptom provocation tasks before and after symptom improvement: a functional magnetic resonance imaging study. *Biol Psychiatry, 57*(8), 901-910. doi:10.1016/j.biopsych.2004.12.039

Niu, Q., Yang, L., Song, X., Chu, C., Liu, H., Zhang, L., . . . Li, Y. (2017). Abnormal resting-state brain activities in patients with first-episode obsessive-compulsive disorder. *Neuropsychiatr Dis Treat, 13*, 507-513. doi:10.2147/NDT.S117510

Norman, L. J., Carlisi, C. O., Christakou, A., Cubillo, A., Murphy, C. M., Chantiluke,

K., . . . Rubia, K. (2017). Shared and disorder-specific task-positive and default mode network dysfunctions during sustained attention in paediatric Attention-Deficit/Hyperactivity Disorder and obsessive/compulsive disorder. *Neuroimage Clin, 15*, 181-193. doi:10.1016/j.nicl.2017.04.013

O'Neill, J., Lai, T. M., Sheen, C., Salgari, G. C., Ly, R., Armstrong, C., . . . Feusner, J. D. (2016). Cingulate and thalamic metabolites in obsessive-compulsive disorder. *Psychiatry Res Neuroimaging, 254*, 34-40. doi:10.1016/j.pscychresns.2016.05.005

Palaniyappan, L., Simmonite, M., White, T. P., Liddle, E. B., & Liddle, P. F. (2013). Neural primacy of the salience processing system in schizophrenia. *Neuron, 79*(4), 814-828. doi:10.1016/j.neuron.2013.06.027

Pizzagalli, D. A. (2011). Frontocingulate dysfunction in depression: toward biomarkers of treatment response. *Neuropsychopharmacology, 36*(1), 183-206. doi:10.1038/npp.2010.166

Qiu, L., Fu, X., Wang, S., Tang, Q., Chen, X., Cheng, L., . . . Tian, L. (2017). Abnormal regional spontaneous neuronal activity associated with symptom severity in treatment-naive patients with obsessive-compulsive disorder revealed by resting-state functional MRI. *Neurosci Lett, 640*, 99-104. doi:10.1016/j.neulet.2017.01.024

Riesel, A., Endrass, T., Kaufmann, C., & Kathmann, N. (2011). Overactive error-related brain activity as a candidate endophenotype for obsessive-compulsive disorder: evidence from unaffected first-degree relatives. *Am J Psychiatry, 168*(3), 317-324. doi:10.1176/appi.ajp.2010.10030416

Rosenberg, D. R., Mirza, Y., Russell, A., Tang, J., Smith, J. M., Banerjee, S. P., . . . Moore, G. J. (2004). Reduced anterior cingulate glutamatergic concentrations in childhood OCD and major depression versus healthy controls. *J Am Acad Child Adolesc Psychiatry, 43*(9), 1146-1153. doi:10.1097/01.chi.0000132812.44664.2d

Saad, Z. S., Gotts, S. J., Murphy, K., Chen, G., Jo, H. J., Martin, A., & Cox, R. W. (2012). Trouble at rest: how correlation patterns and group differences become distorted after global signal regression. *Brain Connect, 2*(1), 25-32. doi:10.1089/brain.2012.0080

Savage, C. R., Deckersbach, T., Wilhelm, S., Rauch, S. L., Baer, L., Reid, T., & Jenike, M. A. (2000). Strategic processing and episodic memory impairment in obsessive compulsive disorder. *Neuropsychology, 14*(1), 141-151.

Saxena, S., Brody, A. L., Schwartz, J. M., & Baxter, L. R. (1998). Neuroimaging and frontal-subcortical circuitry in obsessive-compulsive disorder. *Br J Psychiatry Suppl*(35), 26-37.

Saxena, S., & Rauch, S. L. (2000). Functional neuroimaging and the neuroanatomy of obsessive-compulsive disorder. *Psychiatr Clin North Am, 23*(3), 563-586.

Schlosser, R. G., Wagner, G., Schachtzabel, C., Peikert, G., Koch, K., Reichenbach, J. R., & Sauer, H. (2010). Fronto-cingulate effective connectivity in obsessive compulsive disorder: a study with fMRI and dynamic causal modeling. *Hum Brain Mapp, 31*(12), 1834-1850. doi:10.1002/hbm.20980

Seth, A. K., Barrett, A. B., & Barnett, L. (2015). Granger causality analysis in

neuroscience and neuroimaging. *J Neurosci, 35*(8), 3293-3297. doi:10.1523/JNEUROSCI.4399-14.2015

Shackman, A. J., Salomons, T. V., Slagter, H. A., Fox, A. S., Winter, J. J., & Davidson, R. J. (2011). The integration of negative affect, pain and cognitive control in the cingulate cortex. *Nat Rev Neurosci, 12*(3), 154-167. doi:10.1038/nrn2994

Simon, D., Adler, N., Kaufmann, C., & Kathmann, N. (2014). Amygdala hyperactivation during symptom provocation in obsessive-compulsive disorder and its modulation by distraction. *Neuroimage Clin, 4*, 549-557. doi:10.1016/j.nicl.2014.03.011

Stephan, K. E., Penny, W. D., Moran, R. J., den Ouden, H. E., Daunizeau, J., & Friston, K. J. (2010). Ten simple rules for dynamic causal modeling. *Neuroimage, 49*(4), 3099-3109. doi:10.1016/j.neuroimage.2009.11.015

Stern, E. R., Welsh, R. C., Gonzalez, R., Fitzgerald, K. D., Abelson, J. L., & Taylor, S. F. (2013). Subjective uncertainty and limbic hyperactivation in obsessive-compulsive disorder. *Hum Brain Mapp, 34*(8), 1956-1970. doi:10.1002/hbm.22038

Swartz, J. R., Phan, K. L., Angstadt, M., Klumpp, H., Fitzgerald, K. D., & Monk, C. S. (2014). Altered activation of the rostral anterior cingulate cortex in the context of emotional face distractors in children and adolescents with anxiety disorders. *Depress Anxiety, 31*(10), 870-879. doi:10.1002/da.22289

Tadayonnejad, R., Deshpande, R., Ajilore, O., Moody, T., Morfini, F., Ly, R., . . . Feusner, J. D. (2018). Pregenual Anterior Cingulate Dysfunction Associated with Depression in OCD: An Integrated Multimodal fMRI/(1)H MRS Study. *Neuropsychopharmacology, 43*(5), 1146-1155. doi:10.1038/npp.2017.249

Tang, W., Zhu, Q., Gong, X., Zhu, C., Wang, Y., & Chen, S. (2016). Cortico-striato-thalamo-cortical circuit abnormalities in obsessive-compulsive disorder: A voxel-based morphometric and fMRI study of the whole brain. *Behav Brain Res, 313*, 17-22. doi:10.1016/j.bbr.2016.07.004

Valdes-Sosa, P. A., Roebroeck, A., Daunizeau, J., & Friston, K. (2011). Effective connectivity: influence, causality and biophysical modeling. *Neuroimage, 58*(2), 339-361. doi:10.1016/j.neuroimage.2011.03.058

Ward, L. M. (2013). The thalamus: gateway to the mind. *Wiley Interdiscip Rev Cogn Sci, 4*(6), 609-622. doi:10.1002/wcs.1256

Weber, A. M., Soreni, N., Stanley, J. A., Greco, A., Mendlowitz, S., Szatmari, P., . . . Noseworthy, M. D. (2014). Proton magnetic resonance spectroscopy of prefrontal white matter in psychotropic naive children and adolescents with obsessive-compulsive disorder. *Psychiatry Res, 222*(1-2), 67-74. doi:10.1016/j.pscychresns.2014.02.004

Weidt, S., Lutz, J., Rufer, M., Delsignore, A., Jakob, N. J., Herwig, U., & Bruehl, A. B. (2016). Common and differential alterations of general emotion processing in obsessive-compulsive and social anxiety disorder. *Psychol Med, 46*(7), 1427-1436. doi:10.1017/S0033291715002998

Xie, C., Ma, L., Jiang, N., Huang, R., Li, L., Gong, L., . . . Zhang, Z. (2017). Imbalanced functional link between reward circuits and the cognitive control system in patients with obsessive-compulsive disorder. *Brain Imaging Behav, 11*(4), 1099-

1109. doi:10.1007/s11682-016-9585-7

Yan, C. G., Cheung, B., Kelly, C., Colcombe, S., Craddock, R. C., Di Martino, A., . . . Milham, M. P. (2013). A comprehensive assessment of regional variation in the impact of head micromovements on functional connectomics. *Neuroimage, 76*, 183-201. doi:10.1016/j.neuroimage.2013.03.004

Yucel, M., Wood, S. J., Wellard, R. M., Harrison, B. J., Fornito, A., Pujol, J., . . . Pantelis, C. (2008). Anterior cingulate glutamate-glutamine levels predict symptom severity in women with obsessive-compulsive disorder. *Aust N Z J Psychiatry, 42*(6), 467-477. doi:10.1080/00048670802050546

Zang, Z. X., Yan, C. G., Dong, Z. Y., Huang, J., & Zang, Y. F. (2012). Granger causality analysis implementation on MATLAB: a graphic user interface toolkit for fMRI data processing. *J Neurosci Methods, 203*(2), 418-426. doi:10.1016/j.jneumeth.2011.10.006

Zhang, Z., Fan, Q., Zhu, Y., Tan, L., Chen, Y., Gao, R., . . . Xiao, Z. (2017). Intrinsic functional connectivity alteration of dorsal and rostral anterior cingulate cortex in obsessive-compulsive disorder: A resting fMRI study. *Neurosci Lett, 654*, 86-92. doi:10.1016/j.neulet.2017.06.026

Zuo, C., Ma, Y., Sun, B., Peng, S., Zhang, H., Eidelberg, D., & Guan, Y. (2013). Metabolic imaging of bilateral anterior capsulotomy in refractory obsessive compulsive disorder: an FDG PET study. *J Cereb Blood Flow Metab, 33*(6), 880-887. doi:10.1038/jcbfm.2013.23

Table 1. Demographic and clinical characteristics of patients with obsessive compulsive disorder and healthy controls.

	OCD (n=31)	Controls (n=36)	*P* value
Age, years	27.1±9.5	24.6±7.4	0.773
Gender, male/female	19/12	21/15	0.806
Education, years	13.7±2.9	13.3±2.8	0.588
Illness duration, years	6.0±5.4	-	-
Total YBOCS score	22.9±5.2	-	-
Obsessive subscale score	17.2±4.5	-	-
Compulsive subscale score	5.8±5.8	-	-
HARS	7.9±3.1	-	-
HDRS	9.8±2.7	-	-

Note: for the patients with OCD, the range of total score of Y-BOCS was 16-33 and the range of the obsessive and compulsive subscale scores was 10-28 and 0-16, respectively; the range of HARS scores was 3-19 (from normal level to moderate anxiety) and the range of HDRS scores was 5-17 (from normal level to moderate depression). Mean values ± standard deviation unless stated.

Abbreviations: OCD, obsessive compulsive disorder; Y-BOCS, Yale-Brown Obsessive Compulsive Scale; HARS, 14-item Hamilton Anxiety Rating Scale; HDRS, 17-item Hamilton Depression Rating Scale.

Table 2. One-sample *t*-tests (voxel-level uncorrected $P < 0.001$ and cluster-level uncorrected $P < 0.05$) of normal controls and patients with obsessive compulsive disorder (OCD), respectively, for the driving effects FROM the left pregenual anterior cingulate cortex (pACC) to the whole brain. Regions listed are at peak maxima of clusters in the Montreal Neurological Institute (MNI) space.

The results from the data WITH global signal regression (panel a)						The results from the data WITHOUT global signal regression (panel b)					
Regions	MNI			Cluster size	*t*	Regions	MNI			Cluster size	*t*
	x	y	z	(voxels)	value		x	y	z	(voxels)	value
Positive causal outflow FROM the left pACC to the whole brain											
Controls						**Controls**					
Bilateral caudate and rostral ACC	-12	24	-3	108	7.40	Bilateral caudate, rostral ACC, thalamus, posterior	-15	30	-3	1639	8.18
Left dorsal superior frontal gyrus	-24	-9	63	137	5.87	cingulate cortex, and dorsal superior frontal gyrus					
Bilateral posterior cingulate cortex	-3	-39	24	130	5.75	Bilateral dorsal medial superior frontal gyrus	3	42	60	103	5.68
Right dorsal superior frontal gyrus	30	3	57	66	5.54	Bilateral medial prefrontal cortex	-3	66	18	62	4.98
Bilateral thalamus	0	-6	9	47	5.17	Bilateral precuneus	-3	-72	42	71	4.24
Bilateral precuneus	-3	72	39	173	4.71						
Patients with OCD						**Patients with OCD**					
Bilateral caudate and rostral ACC	-6	18	3	88	6.79	Bilateral dorsal medial prefrontal cortex	3	54	48	340	7.75
Bilateral ventral medial prefrontal cortex	3	51	12	27	5.62	Bilateral caudate and rostral ACC	-15	21	12	376	6.48
Bilateral dorsal medial prefrontal cortex	-3	48	48	53	5.16	Cerebellar vermis	0	-42	3	56	5.32
Cerebellar vermis	0	-63	-9	20	4.94	Bilateral ventral medial prefrontal cortex	0	57	12	110	4.85
Negative causal outflow FROM the left pACC to the whole brain											
Controls						**Controls**					
Right middle frontal gyrus	39	51	24	33	6.1	Right supramarginal gyrus	66	-18	24	1215	6.6
Left medial temporal gyrus and left cerebellum	-39	-36	-33	68	5.43	Left supramarginal gyrus	-66	-36	33	512	6.4
Left orbitofrontal cortex	-39	30	-9	84	5.17	Right superior parietal lobule	42	-51	63	202	5.77
Right inferior frontal gyrus	51	24	6	34	4.75	Right anterior insular, middle and inferior frontal gyrus	42	51	21	764	5.57
Right anterior insular and orbitofrontal cortex	36	18	-12	34	4.43	Left orbitofrontal cortex	-36	30	-12	108	5.3
Right supramarginal gyrus	66	-15	27	165	4.36	Left medial temporal gyrus and left cerebellum	-36	-42	-27	120	5.27
Left supramarginal gyrus	-63	-39	36	32	4.25	Left occipital lobe	-33	-72	-3	439	4.91
Right inferior temporal gyrus and right cerebellum	39	-39	-27	44	4.24	Right occipital lobe	24	-84	18	194	4.25
Patients with OCD						**Patients with OCD**					
Right inferior temporal gyrus	45	-33	-21	24	4.29	Left superior parietal lobule	-48	-45	60	139	5.97
Left medial temporal gyrus	-42	-39	-21	73	4.14	Right middle frontal gyrus	51	48	15	26	4.48
Right middle frontal gyrus	51	45	15	56	3.88	Right superior parietal lobule	51	-33	60	23	4.22
Left orbitofrontal cortex	-42	27	-9	42	3.81	Left orbitofrontal cortex	-45	15	-6	19	3.93

Table 3. One-sample *t*-tests (voxel-level uncorrected $P < 0.001$ and cluster-level uncorrected $P < 0.05$) of normal controls and patients with obsessive compulsive disorder (OCD), respectively, for feedback effects from the whole brain TO the left pregenual anterior cingulate cortex (pACC). Regions listed are at peak maxima of clusters in the Montreal Neurological Institute (MNI) space.

The results from the data WITH global signal regression (panel a)						The results from the data WITHOUT global signal regression (panel b)					
Regions	MNI			Cluster size	*t*	Regions	MNI			Cluster size	*t*
	x	y	z	(voxels)	value		x	y	z	(voxels)	value
Positive causal inflow from the whole brain TO the left pACC											
Controls						**Controls**					
Left supramarginal gyrus	-57	-39	27	20	5.6	Right inferior frontal gyrus	48	27	0	104	5.42
Left cerebellum	-42	-42	-36	42	5.32	Right supramarginal gyrus	69	-24	36	105	4.75
Left medial temporal gyrus	-30	-36	-9	71	5.29	Left supramarginal gyrus	-57	-39	30	54	4.47
Right cerebellum	24	-72	-48	39	5	Left insular	-39	0	-6	33	3.98
Right medial temporal gyrus	42	-39	-27	55	4.79	Left medial temporal gyrus	-30	-42	-12	20	3.65
Right supramarginal gyrus	63	-18	24	19	4.24						
Patients with OCD						**Patients with OCD**					
Left medial temporal gyrus	-33	-33	-18	25	4.09	Left inferior frontal gyrus	-57	-12	21	155	4.71
Right cerebellum	18	-75	-45	36	3.83	Left medial temporal gyrus	-30	-51	-6	80	4.44
Right medial temporal gyrus	45	-36	-21	29	3.8	Right temporal pole	30	12	-45	40	3.81
						Right inferior frontal gyrus	63	-9	21	34	3.6
						Right medial temporal gyrus	30	-36	-15	19	3.41
Negative causal inflow from the whole brain TO the left pACC											
Controls						**Controls**					
Bilateral thalamus	0	-3	12	23	5.02	Bilateral caudate and thalamus	-15	30	-3	1160	7.74
Right dorsal superior frontal gyrus	12	15	54	74	5.01	Bilateral dorsal medial superior frontal gyrus	0	54	48	99	5.46
Bilateral posterior cingulate cortex	0	-30	27	27	4.61	Bilateral ventral medial and left ventral superior	-3	69	12	75	5.21
Bilateral precuneus	0	-81	42	93	4.54	frontal gyrus					
Left inferior parietal lobule	-36	-57	45	31	4.33	Left middle frontal gyrus	-33	0	66	31	3.88
Left middle frontal gyrus	-30	0	57	31	4.27	Cerebellar vermis and posterior cingulate cortex	-6	-39	-3	92	4.55
Cerebellar vermis	0	-75	-9	27	4.08	Bilateral precuneus	3	-81	42	37	3.84
Left ventral superior frontal gyrus	-24	57	6	36	3.82						
Patients with OCD						**Patients with OCD**					
Bilateral dorsal medial prefrontal cortex	0	48	45	56	4.98	Bilateral occipital lobe	18	-93	-15	134	6.78
Bilateral ventral medial prefrontal cortex	0	48	12	74	4.87	Bilateral dorsal and ventral medial prefrontal cortex	6	54	45	473	6.73
Bilateral caudate and rostral ACC	-6	18	3	35	4.44	Right caudate	15	20	6	160	6.23
Cerebellar vermis	0	-63	-6	48	4.01	Left caudate	-12	21	12	50	4.33

Table 4. Differences between patients with obsessive compulsive disorder and controls for amplitude of low-frequency fluctuation and causal influence from and to the left pregenual anterior cingulate cortex.

Regions	MNI			Cluster size	*P*	ALFF value or path coefficient	
	x	y	z	(voxels)	value	Controls	OCD patients
Results from data WITH global signal regression between 31 patients and 36 controls (panel a)							
Amplitude of low-frequency fluctuation							
Left pregenual ACC	-9	39	3	54	0.029	1.56±0.31	1.26±0.21
Causal outflow from left pregenual ACC							
Right dorsal SFG	30	3	54	22	0.016	1.27±1.6	-0.09±1.4
Left precuneus	-12	-69	36	8	0.019	1.51±2.08	-0.16±1.87
Causal inflow to left pregenual ACC							
Left ventral SFG	-24	57	12	20	0.029	-0.68±1.09	0.42±1.06
Results from data WITH global signal regression between 29 adult patients and 36 controls (panel b)							
Amplitude of low-frequency fluctuation							
Left pregenual ACC	-9	39	3	34	0.013	1.46±0.29	1.15±0.17
Causal outflow from left pregenual ACC							
Right dorsal SFG	30	3	54	16	0.017	1.13±1.36	0.21±1.32
Left precuneus	-9	-72	39	22	0.027	1.77±2.2	0.51±2.04
Causal inflow to left pregenual ACC							
Left ventral SFG	-24	57	12	21	0.032	-0.68±1.09	0.42±1.04
Results from data WITHOUT global signal regression between 31 patients and 36 controls (panel c)							
Amplitude of low-frequency fluctuation							
Left pregenual ACC	-6	39	9	20	0.045	1.48±0.3	1.26±0.21
Causal outflow from left pregenual ACC							
Right dorsal SFG	15	18	48	21	0.029	0.46±0.86	-0.1±0.83
Left precuneus	-12	-66	39	17	0.039	0.71±1.45	-0.39±1.68
Causal inflow to left pregenual ACC							
Left thalamus and caudate	-6	-6	12	40	0.041	-1.75±1.42	0.22±2.14
Left ventral SFG	-27	63	12	33	0.02	-0.36±0.77	0.18±0.65

Regions listed are at peak maxima of clusters in the Montreal Neurological Institute (MNI) space. amplitude of low-frequency fluctuation (ALFF) values and path coefficients are given as mean value ± standard deviation. *P* values calculated by 2-sample *t*-test, family-wise error corrected $P < 0.05$ at cluster level.

Abbreviations: ACC, anterior cingulate cortex; OCD, obsessive compulsive disorder; SFG, superior frontal gyrus.

Figure Legends

Figure 1. In (a) the blue area shows the location of lower amplitude of low-frequency fluctuations in the left pregenual anterior cingulate cortex (pACC) in patients than controls. In (e) there are reduced driving effects of Granger causality effective connectivity (blue arrow, meaning a less excitatory influence) from the left pACC to the right dorsal superior frontal gyrus (SFG) (also shown in panel b) and to the left precuneus (also shown in panel c), respectively; greater feedback effect (red arrow, meaning a less inhibitory influence) from the left ventral SFG (also shown in panel d) to the left pACC in patients compared to controls.

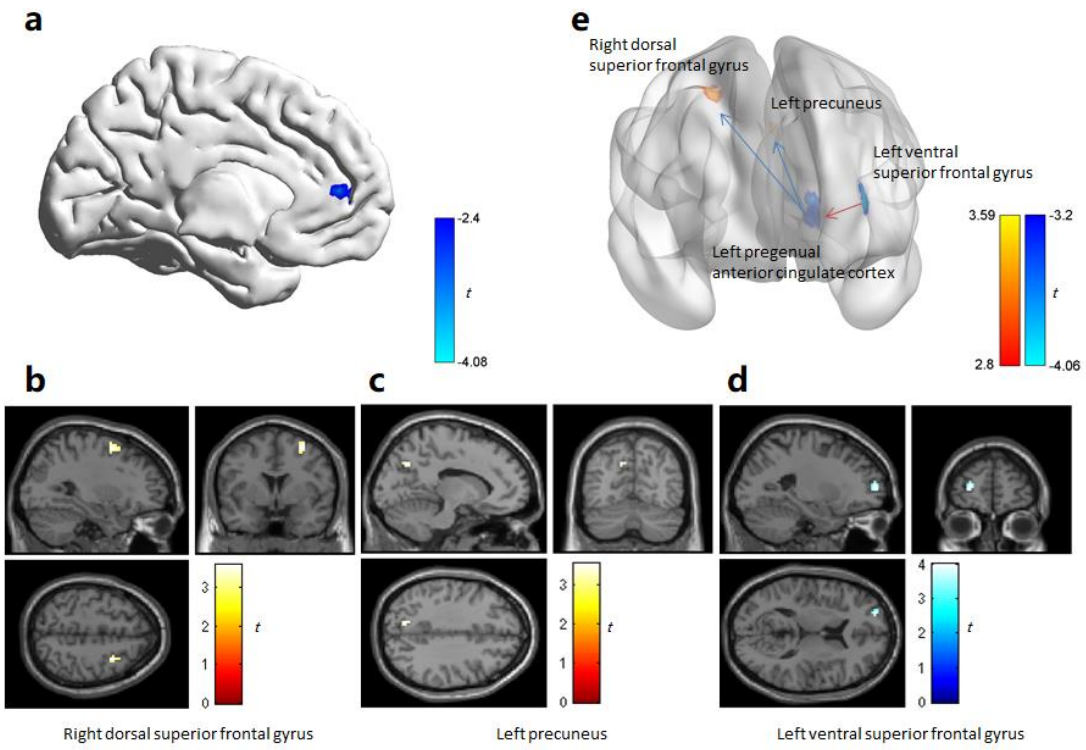

Figure 2. The effective connectivity of Granger causality analysis from the left pregenual anterior cingulate cortex (ACC) to the whole brain in patients and controls, respectively. The within group results of 1-sample *t*-tests are from the data with (a) and without (b) global signal regression, respectively.

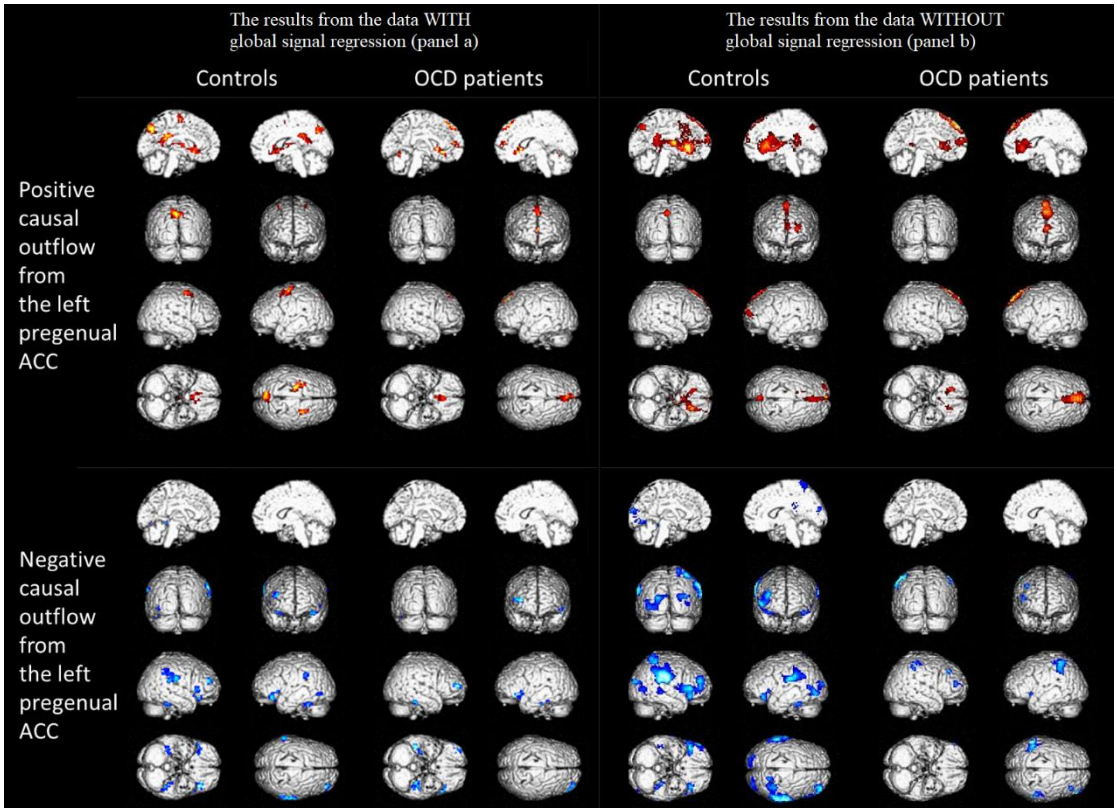

Figure 3. The effective connectivity of Granger causality analysis from the whole brain regions to the left pregenual anterior cingulate cortex (ACC) in patients and controls, respectively. The within group results of 1-sample *t*-tests are from the data with (a) and without (b) global signal regression, respectively.

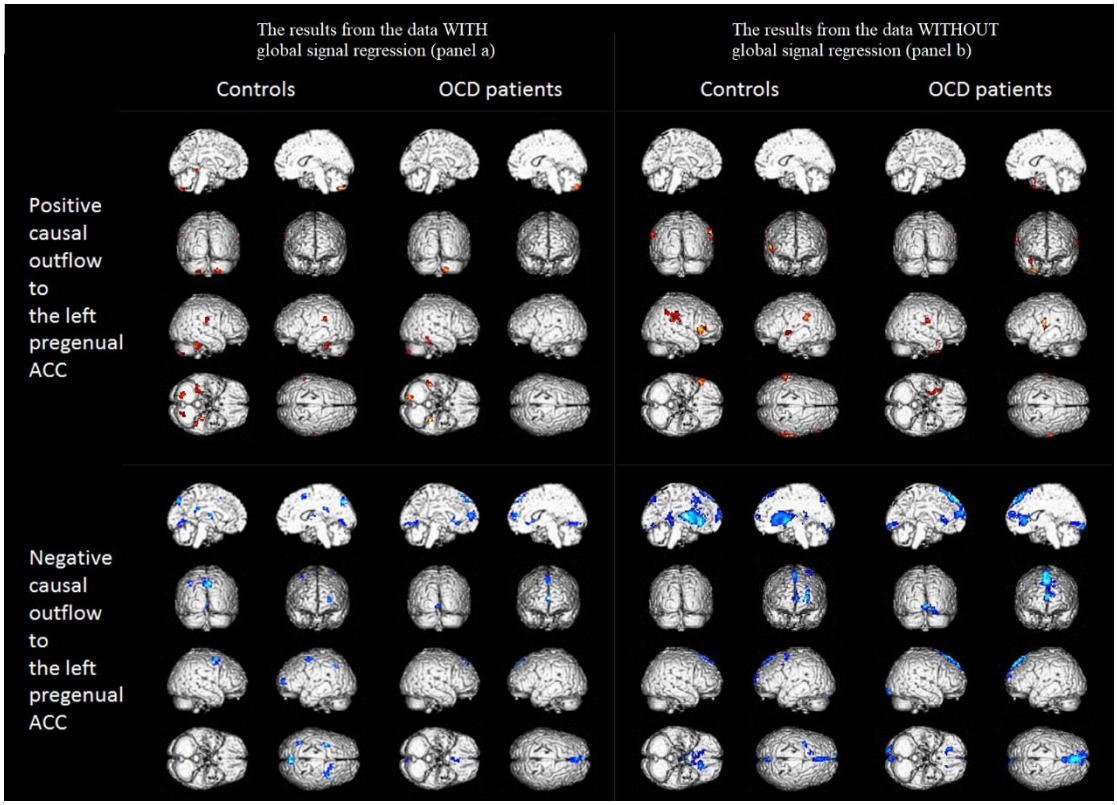

Figure 4. (a) The results of 3-group comparisons regarding amplitude of low-frequency fluctuation (ALFF) and effective connectivity (EC) of left pregenual anterior cingulate cortex (pACC) were consistent with the results compared between all the patients and controls (*, $P < 0.05$; **, $P < 0.001$). (b) The statistical comparisons of 29 adult patients with obsessive compulsive disorder and 36 controls revealed similar group differences in ALFF and EC as seen in the main results. (c) The results from the data without global signal regression are similar to the main results, with additional greater feedback effect from the left thalamus and caudate to the left pACC in patients compared to controls. Abbreviation: d/vSFG, dorsal/ventral superior frontal gyrus. Note: the blue/red arrow in panel c means the same as in Figure 1.